Quantum tomography of the two-lepton system with ALICE

Sára Haidlová

[1]Faculty of Nuclear Sciences and Physical Engineering
Czech Technical University in Prague

September 15, 2023

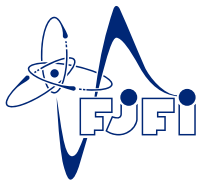

Quantum Tomography

- Describes all observable features of a given quantum mechanical system while bypassing model based formalism.
- This allows for focusing on characterization of experimental data.
- The unknown intermediate state of the system can be parametrized by a density matrix $\rho(X)$ and is being probed described by $\rho(probe)$ that is known from measured variables.
- The Cholesky decomposition of $\rho(X)$ and the connection between angular distribution and cross section allows for density matrix parameter estimation by fitting measured data.

$$\begin{aligned}\frac{dN}{d\Omega} &= \frac{1}{4}(1+m_3^2) \\ &+ \frac{1}{4}(1-3m_3^2)\cos^2\theta \\ &- \frac{1}{2}m_3 m_6 \sin(2\theta)\cos\phi \\ &+ \frac{1}{2}(m_2^2+m_8^2+m_9^2+\frac{1}{2}m_3^2-\frac{1}{2})\sin^2\theta\cos(2\phi) \\ &- \frac{1}{4}(2m_2^2+m_3^2+-1)\sin^2\theta\sin(2\phi).\end{aligned} \tag{1}$$

Quarkonium Polarization

- J/ψ is studied via its decay into dilepton pair.
- Leptons are emitted back-to-back.
- The angular distribution of decay products provides information about polarization or spin alignment.
- It can be parametrized by a set of parameters $\lambda_\theta, \lambda_\varphi, \lambda_{\theta\varphi}, \tilde{\lambda}$.

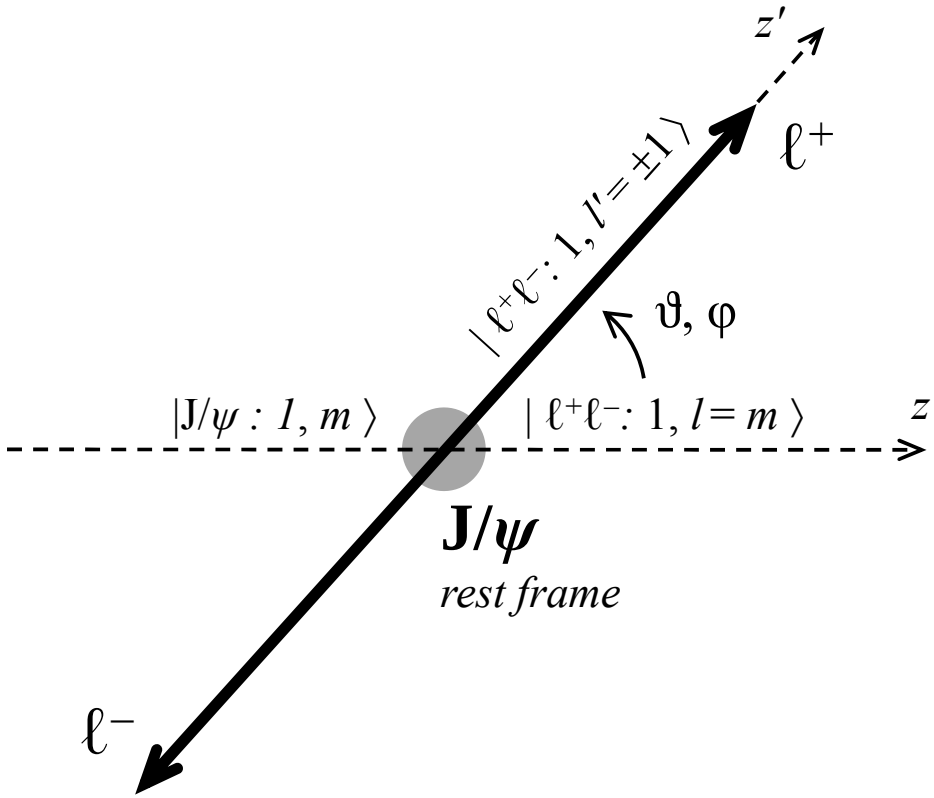

[0] P. Faccioli et al., [arXiv:1006.2738 [hep-ph]]

Quarkonium Polarization

- Electric and magnetic fields of charged particles moving at ultra-relativistic speeds are both perpendicular to the beam directions and they propagate as linearly polarized electromagnetic waves.
- Photons generated by those fields are considered to be linearly polarized in the transverse plane.
- Thus it is expected that produced J/ψ is transversely polarized thanks to helicity conservation.

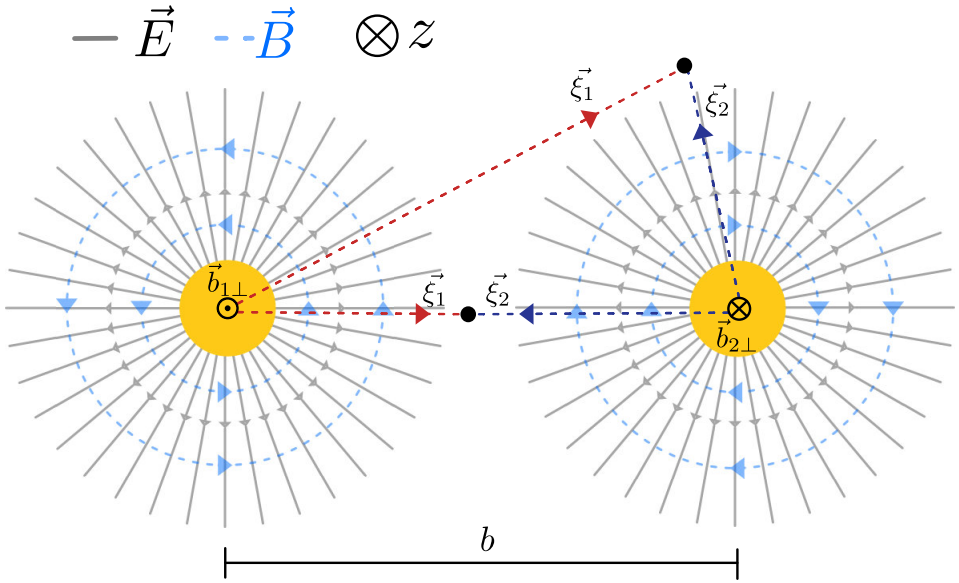

J. D. Brandenburg, W. Zha and Z. Xu, [arXiv:2103.16623 [hep-ph]].

MC analysis

- In order to compare measured sample with an ideal case, a set of Monte Carlo data was generated.
- The data were generated using EvtGen with same energy configuration as the measured sample for both coherent and incoherent photoproduction with three polarization states.

Angular distribution of MC data samples

- The distributions for coherent data sample show strong dependence on angular distribution with clear differences between longitudinal (left) and transversal (right) polarization.

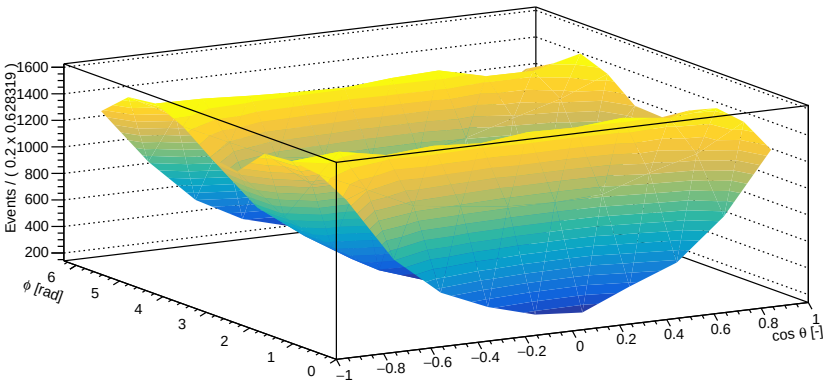

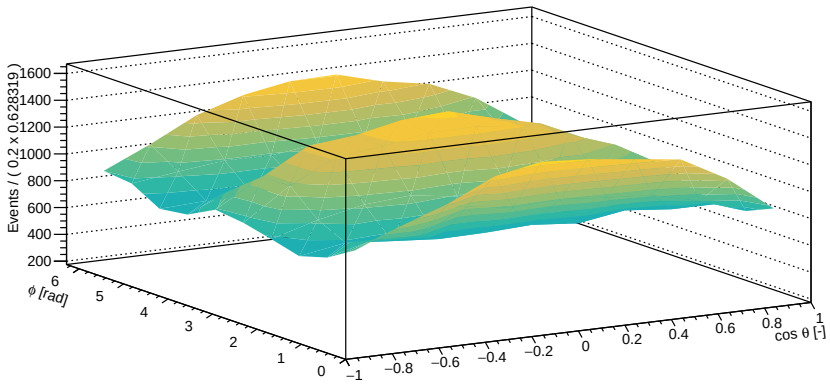

Angular distribution of MC data samples

- The distributions for incoherent data sample show strong dependence on angular distribution with clear differences between longitudinal (left) and transversal (right) polarization.

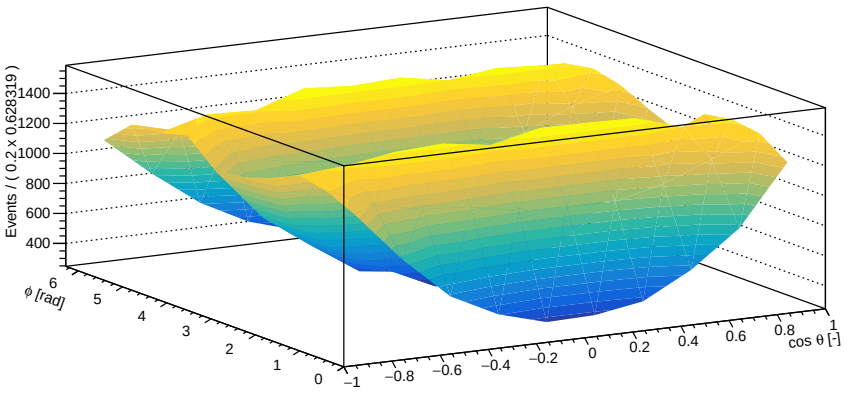

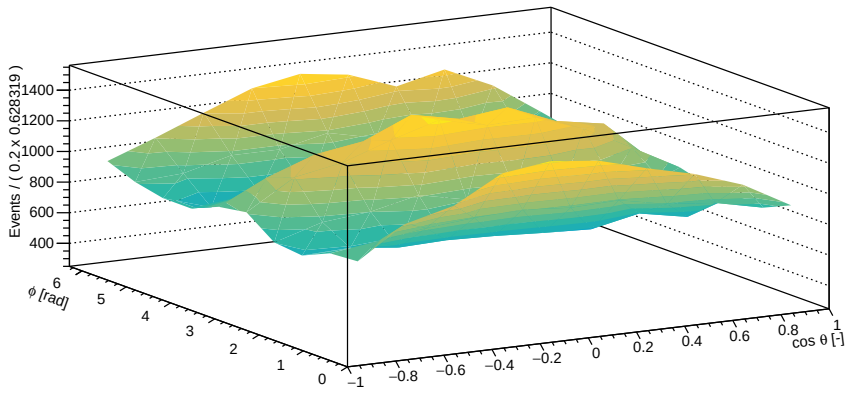

Angular distribution of MC data samples

- The distributions of unpolarized data samples showed no strong dependence for both coherent (left) and incoherent (right) photoproduction.

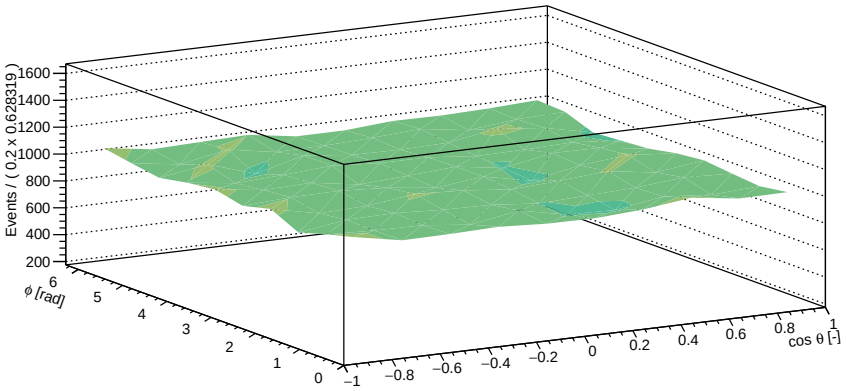

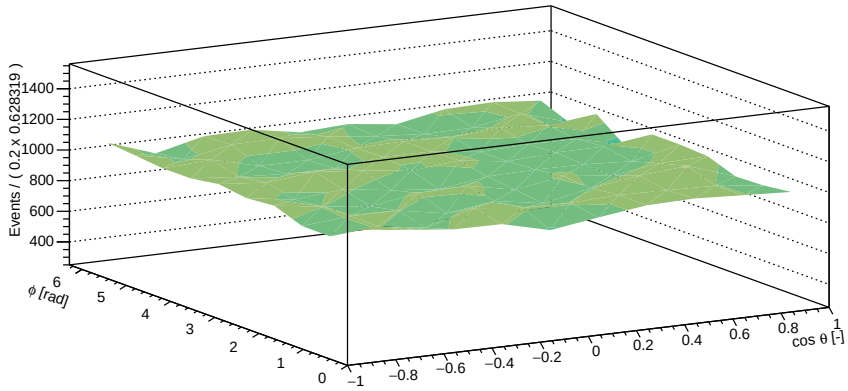

MC data sample analysis

- The analysis of all of the data samples show results compatible with expectations.

Transverse		**Longitudinal**		**Unpolarized**	
λ_θ	-0.3269	λ_θ	0.9998	λ_θ	-0.0083
λ_ϕ	0.3304	λ_ϕ	-0.9429	λ_ϕ	0.1382
$\lambda_{\theta\phi}$	-0.0638	$\lambda_{\theta\phi}$	-0.0131	$\lambda_{\theta\phi}$	-0.4246
$\tilde{\lambda}$	0.9922	$\tilde{\lambda}$	-0.9424	$\tilde{\lambda}$	0.4716

Table: Polarization parameters $\lambda_\theta, \lambda_\phi, \lambda_{\theta\phi}$ and $\tilde{\lambda}$ calculated from fit parameters with frame invariant parameter $\tilde{\lambda}$ for coherent J/ψ.

MC data sample analysis

- The analysis of all of the data samples show results compatible with expectations.

Transverse		**Longitudinal**		**Unpolarized**	
λ_θ	-0.2642	λ_θ	0.9998	λ_θ	-0.0067
λ_ϕ	0.3274	λ_ϕ	-0.8253	λ_ϕ	0.1300
$\lambda_{\theta\phi}$	-0.1601	$\lambda_{\theta\phi}$	-0.0120	$\lambda_{\theta\phi}$	-0.4296
$\tilde{\lambda}$	1.0672	$\tilde{\lambda}$	-0.8087	$\tilde{\lambda}$	0.4408

Table: Polarization parameters $\lambda_\theta, \lambda_\phi, \lambda_{\theta\phi}$ and $\tilde{\lambda}$ calculated from fit parameters with frame invariant parameter $\tilde{\lambda}$ for incoherent J/ψ.

Data selection

- UPC Pb-Pb collisions with $\sqrt{s_{NN}} = 5.02$ TeV measured during 2018 data taking.
- Data selection
  - 2 good tracks in an otherwise empty detector
  - no signal in ADA, ADC, V0A, V0C
  - only muon pairs
  - transverse momentum cut $p_T < 0.2$ GeV/c

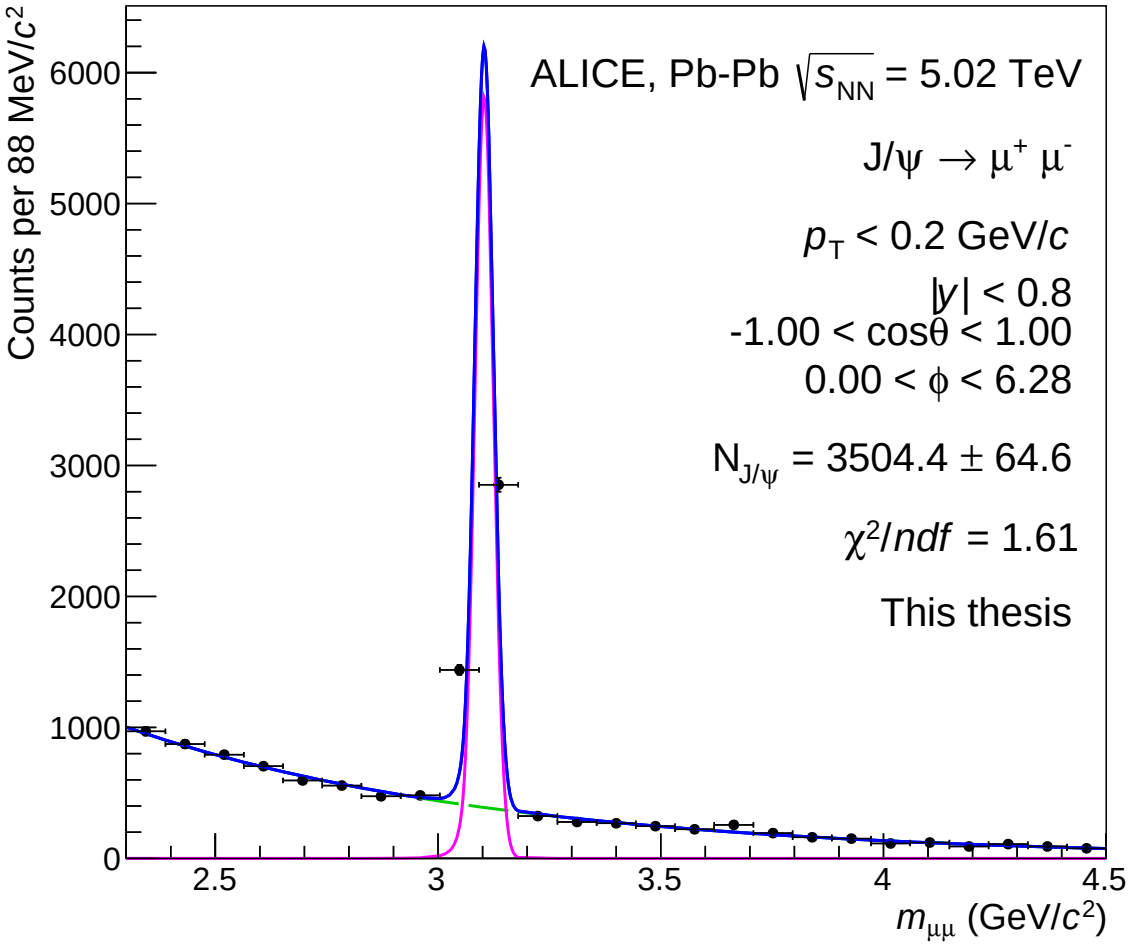

Data selection

- UPC Pb-Pb collisions with $\sqrt{s_{NN}} = 5.02$ TeV measured during 2018 data taking.
- Data selection
  - 2 good tracks in an otherwise empty detector
  - no signal in ADA, ADC, V0A, V0C
  - only muon pairs
  - transverse momentum cut $p_T < 0.2$ GeV/c

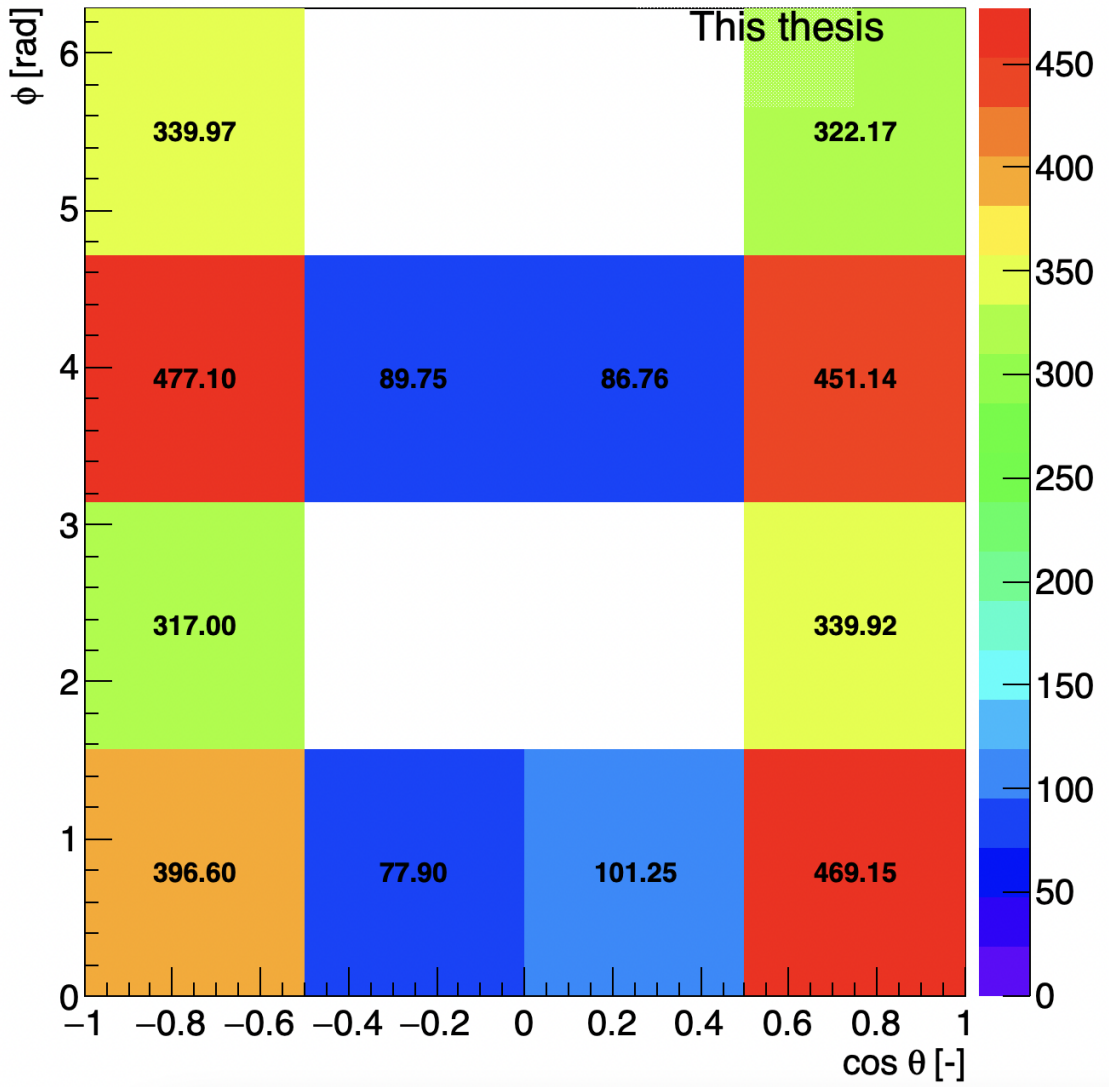

Data selection

- UPC Pb-Pb collisions with $\sqrt{s_{NN}} = 5.02$ TeV measured during 2018 data taking.
- Data selection
  - 2 good tracks in an otherwise empty detector
  - no signal in ADA, ADC, V0A, V0C
  - only muon pairs
  - transverse momentum cut $p_T > 0.2$ GeV/c

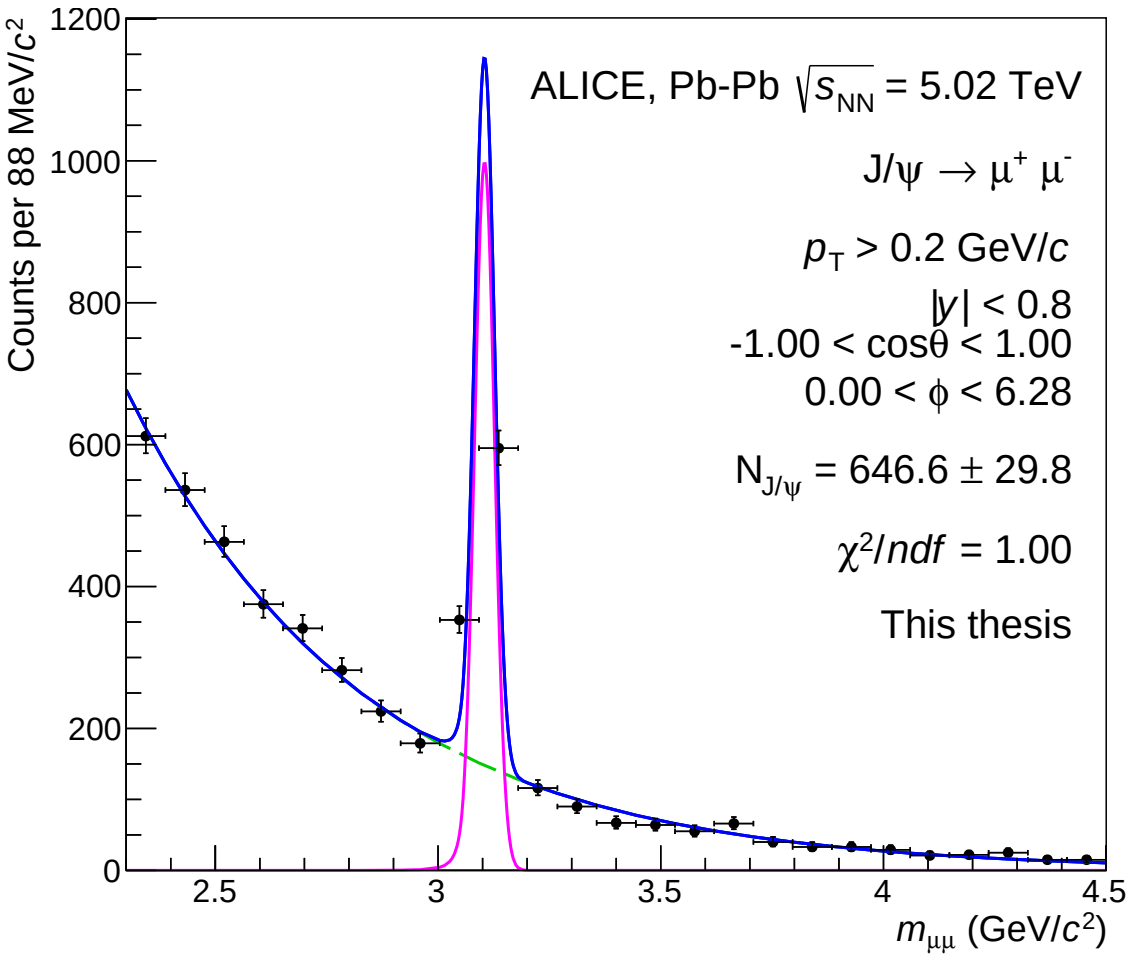

Data selection

- UPC Pb-Pb collisions with $\sqrt{s_{NN}} = 5.02$ TeV measured during 2018 data taking.
- Data selection
  - 2 good tracks in an otherwise empty detector
  - no signal in ADA, ADC, V0A, V0C
  - only muon pairs
  - transverse momentum cut $p_T > 0.2$ GeV/c

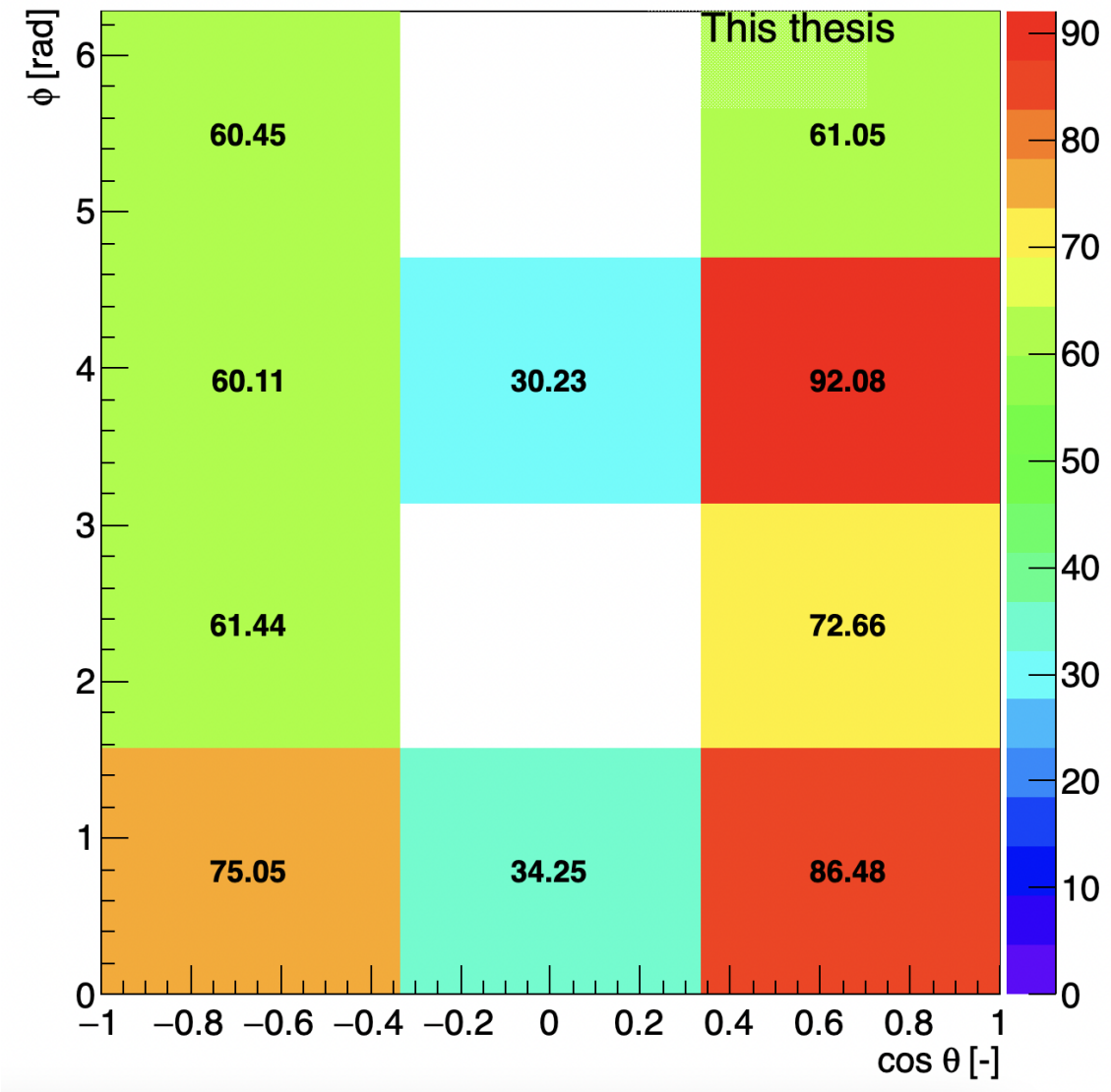

Acceptance

- First step towards correction determination.
- $$Acc = \frac{N_{gen}(\mathrm{y_{cut}}, \eta_{\mathrm{cut}})}{N_{gen}(\mathrm{y_{cut}})} \qquad (2)$$
- A strong dependence in angular distributions lead to shift in ϕ.

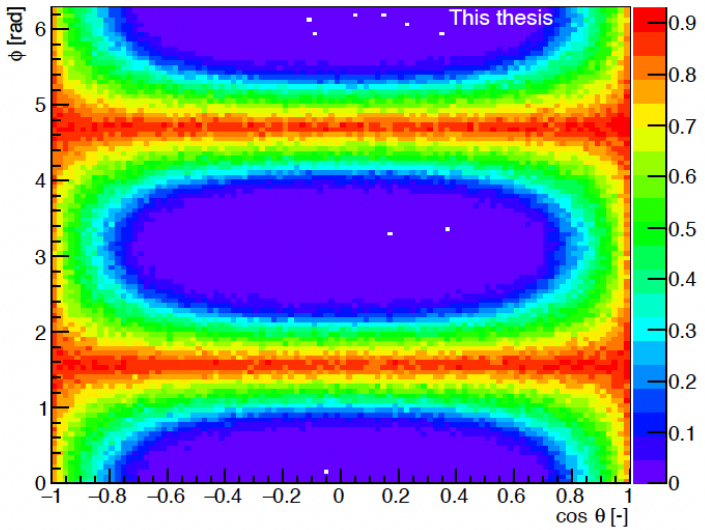

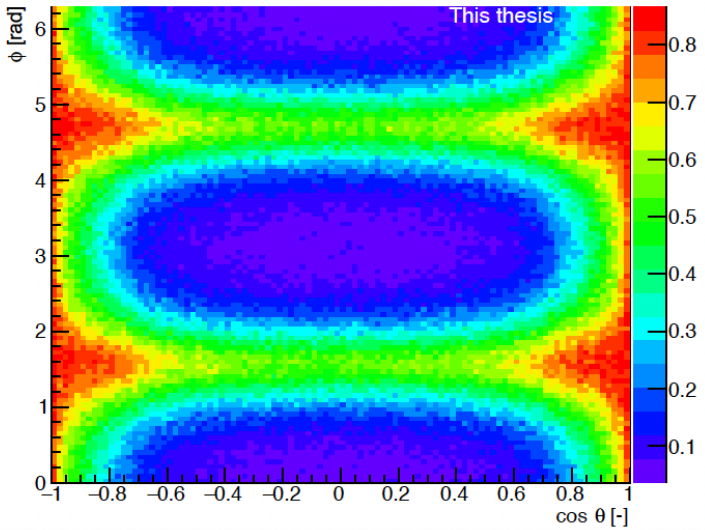

Acceptance

- First step towards correction determination.
- $$Acc = \frac{N_{gen}(\mathrm{y_{cut}}, \eta_{\mathrm{cut}})}{N_{gen}(\mathrm{y_{cut}})} \qquad (3)$$
- A strong dependence in angular distributions lead to shift in ϕ.

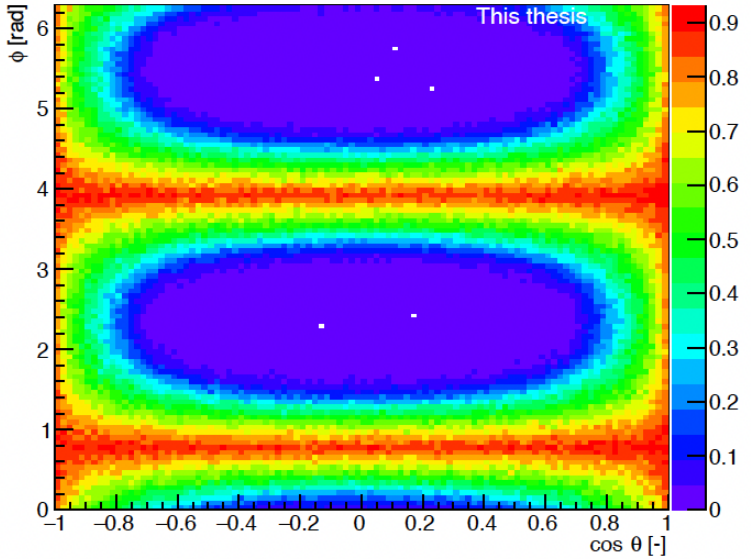

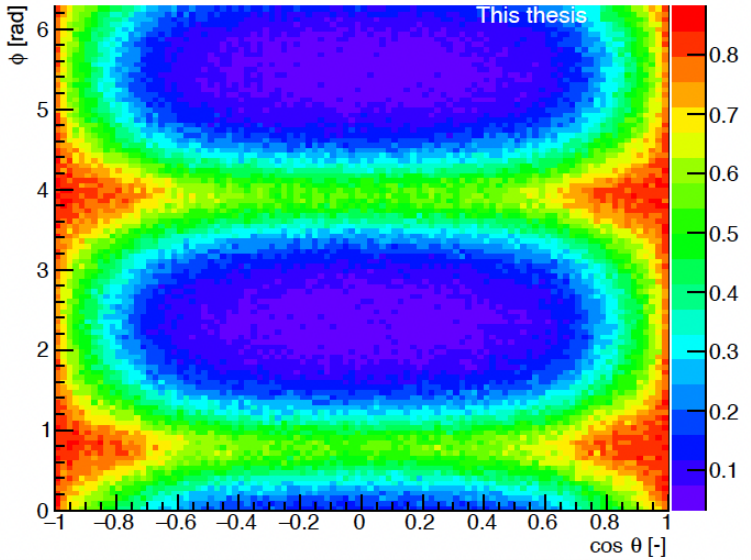

Choice of binning

- The choice of binning depended on the number of events in each bin and the detector resolution.
- The resolution is determined by finding a difference between reconstructed and generated events in $\cos\theta$ and ϕ distributions.
- The resolution is equal to FWHM of the distribution.

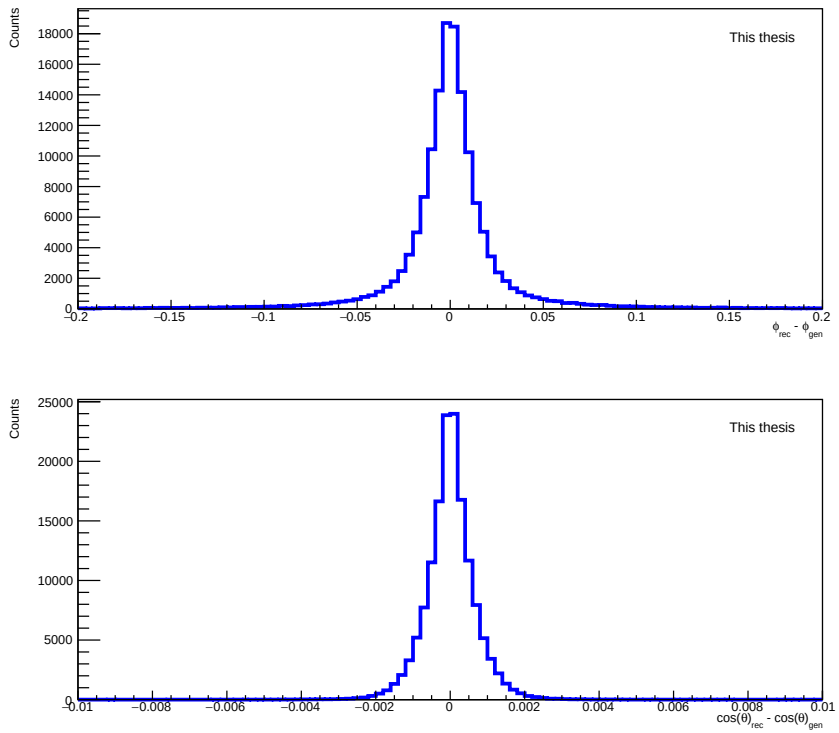

Choice of binning

- The choice of binning depended on the number of events in each bin and the detector resolution.
- The resolution is determined by finding a difference between reconstructed and generated events in $\cos\theta$ and ϕ distributions.
- The resolution is equal to FWHM of the distribution.

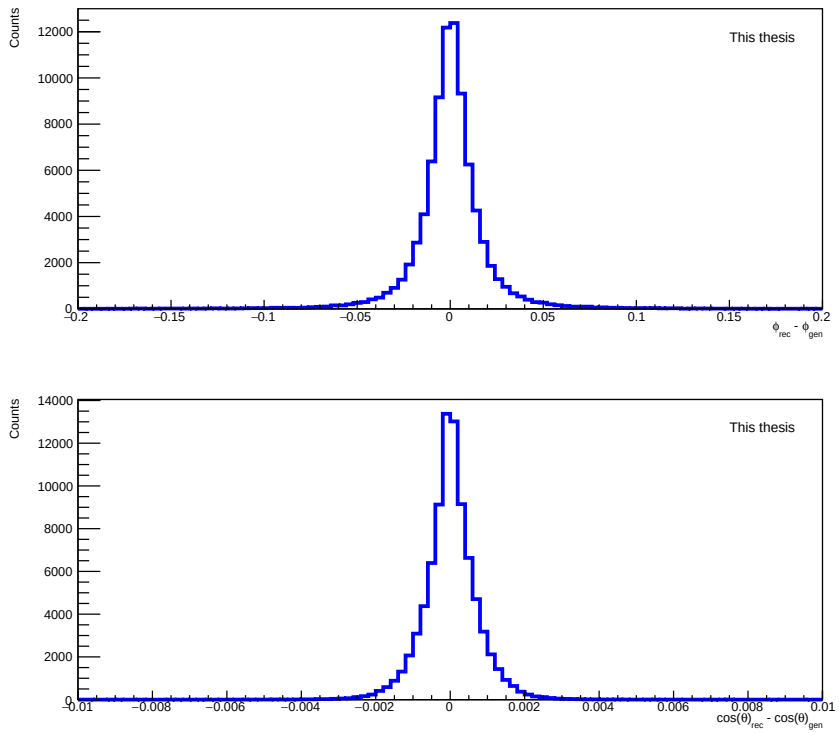

Acceptance and efficiency

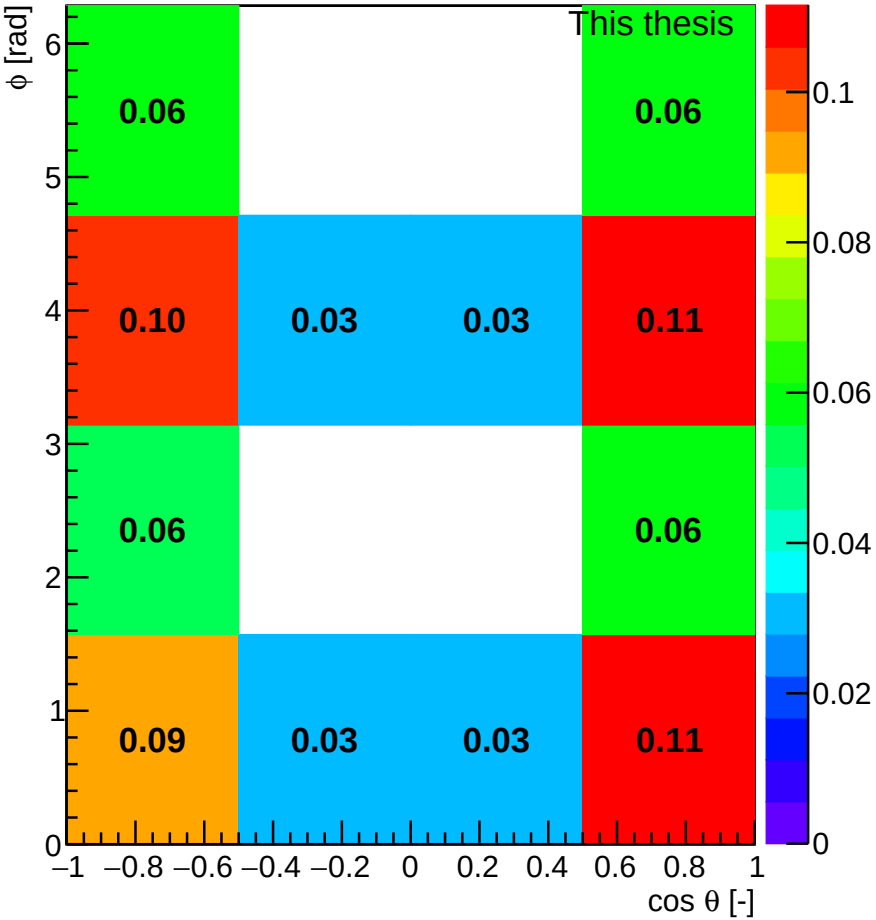

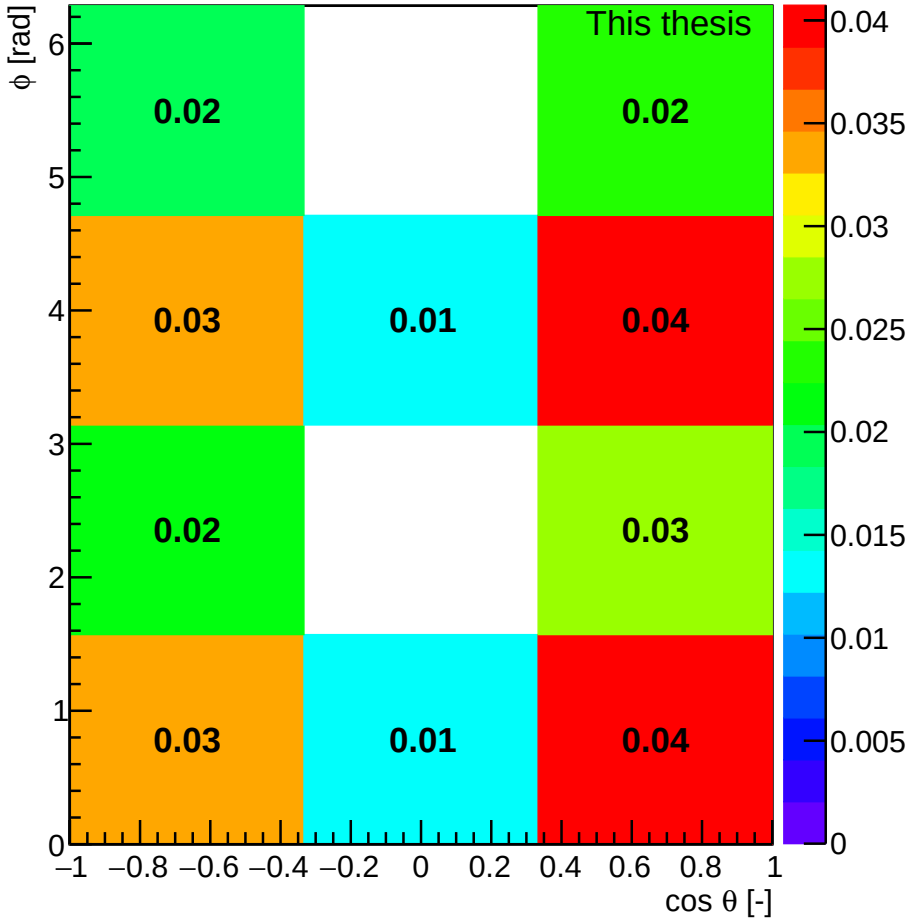

Incoherent contamination

- Coherent and incoherent data are selected using a p_T cut.
- However, it is possible to observe contamination from each data sample that can play a significant role in each of the p_T regions.
-

$$N_{coh} = \frac{N_{yield}^{coh}}{1 + f_I}. \qquad (4)$$

-

$$f_I = \frac{\sigma_{incoh} \frac{N_{rec}^{incoh}(p_T<0,2)}{N_{gen}^{incoh}}}{\sigma_{coh} \frac{N_{rec}^{coh}(p_T<0.2)}{N_{gen}^{coh}}} \qquad (5)$$

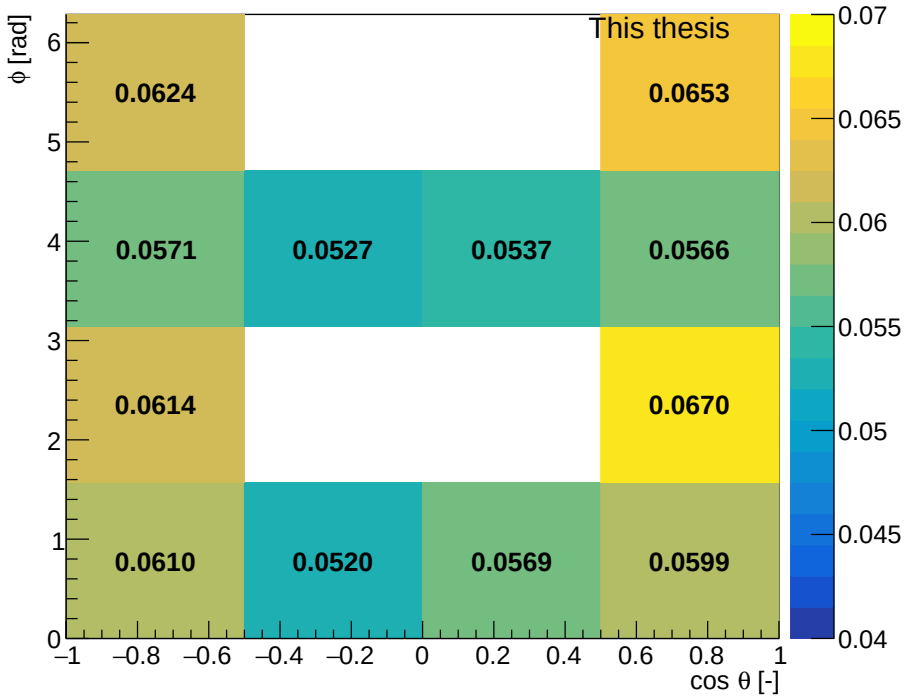

Coherent contamination

- Coherent and incoherent data are selected using a p_T cut.
- However, it is possible to observe contamination from each data sample that can play a significant role in each of the p_T regions.
-

$$N_{incoh} = \frac{N_{yield}^{incoh}}{1 + f_C}, \qquad (6)$$

-

$$f_C = \frac{\sigma_{coh} \frac{N_{rec}^{coh}(p_T > 0{,}2)}{N_{gen}^{coh}}}{\sigma_{incoh} \frac{N_{rec}^{incoh}(p_T > 0.2)}{N_{gen}^{incoh}}} \qquad (7)$$

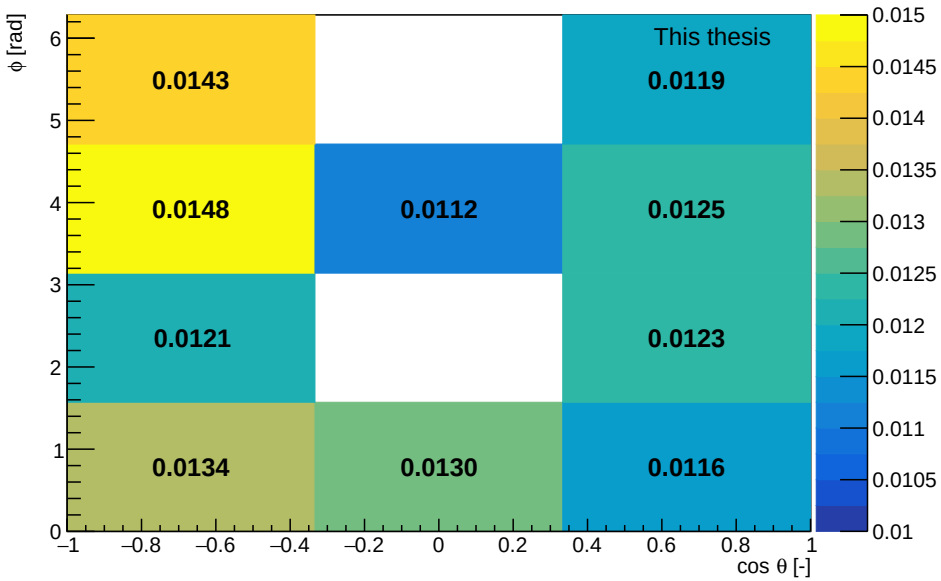

MC parameter estimation

- In order to compare MC data samples with measured data we needed to modify the data sample to resemble the measured one.
- Thus the MC data we fitted in the same regions as the data.

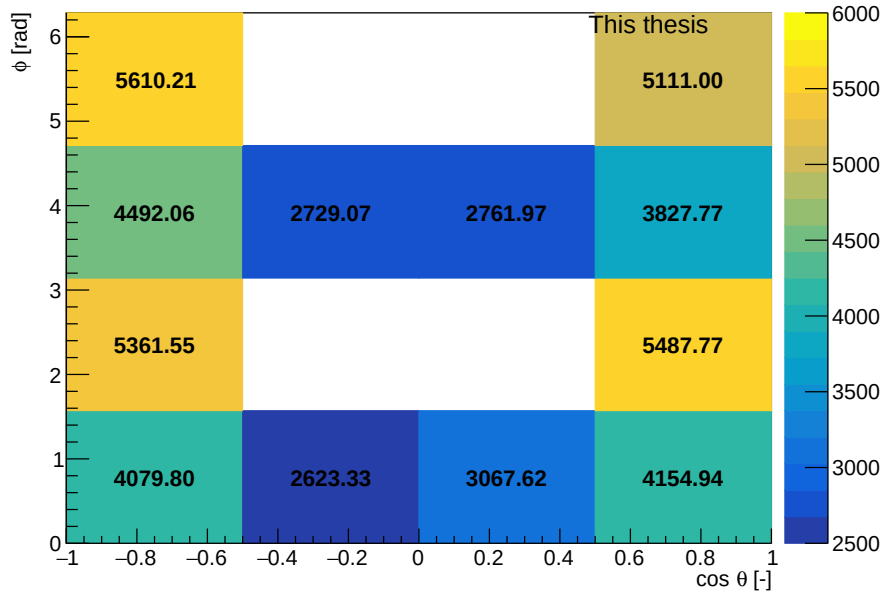

MC parameter estimation

- In order to compare MC data samples with measured data we needed to modify the data sample to resemble the measured one.
- Thus the MC data we fitted in the same regions as the data.
- The data sample was fitted by 1D distributions using projections of two distinct regions, simultaneously.

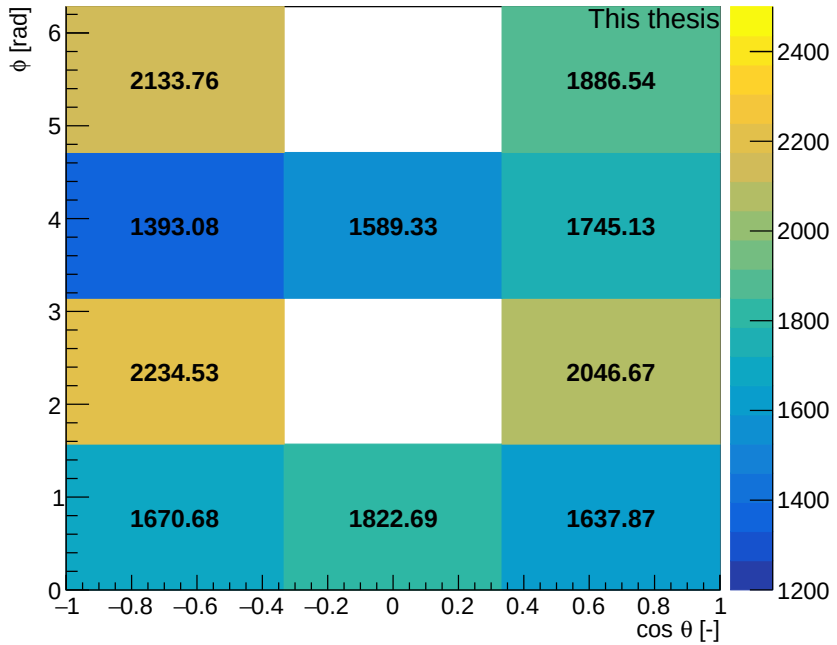

MC density matrix determination - Coherent photoproduction

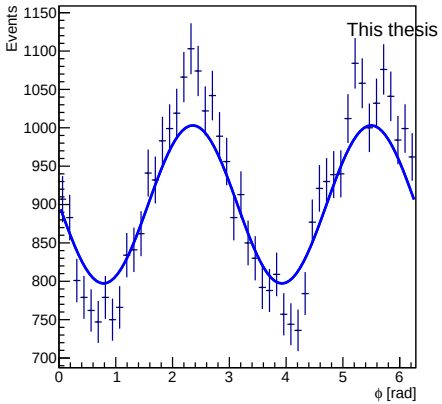

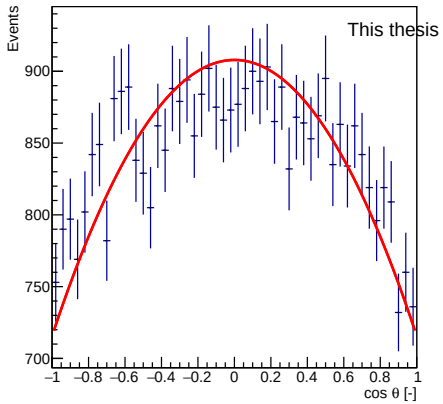

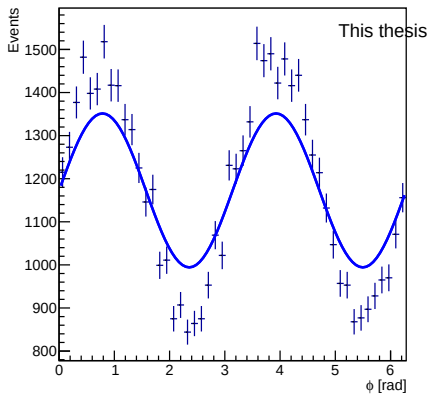

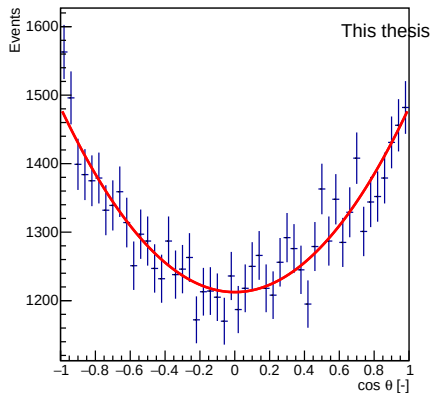

$$\rho_{fit}^{trans} = \begin{pmatrix} 0.000044 & 0 & 0.004807 \\ 0 & 0.479137 & 0 \\ 0.004807 & 0 & 0.520819 \end{pmatrix} \quad (8)$$

$$\rho_{fit}^{long} = \begin{pmatrix} 1 & 0 & 0.00018 \\ 0 & 0 & 0 \\ 0.00018 & 0 & 0 \end{pmatrix} \quad (9)$$

Parameter estimation of measured data

- After applying all corrections the corrected yield was fitted with angular distribution function in two regions.
- The coherent data sample showed nonphysical shape of the distribution.

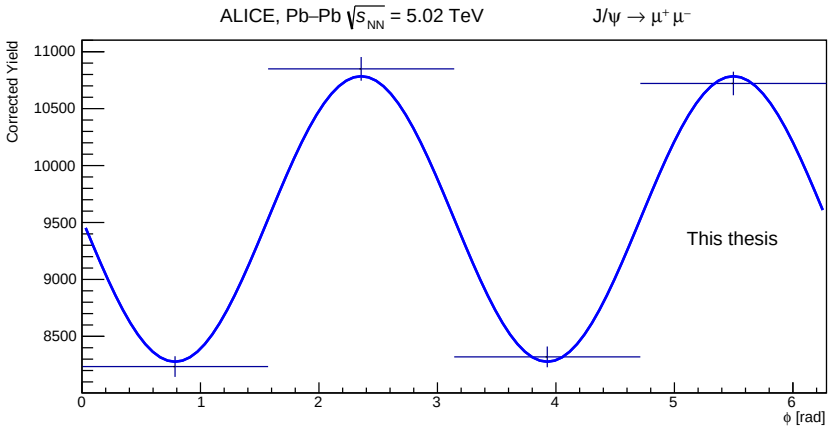

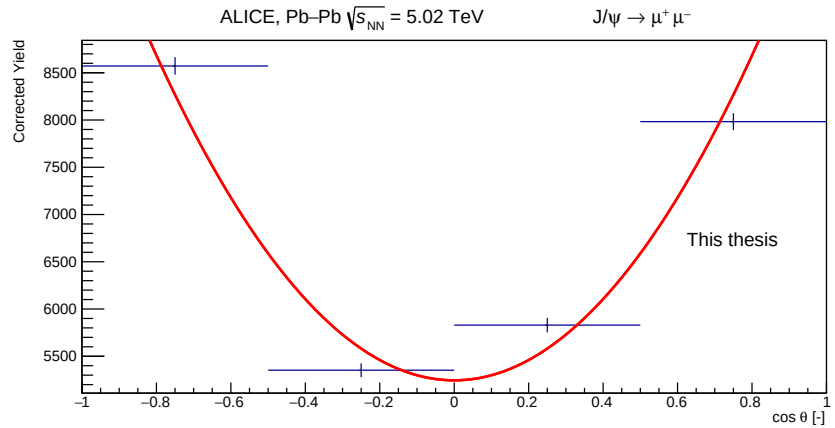

Parameter estimation of measured data

- After applying all corrections the corrected yield was fitted with angular distribution function in two regions.
- The coherent data sample showed nonphysical shape of the distribution.
- The incoherent data sample showed reasonable results to determine the density matrix and values for polarization parameters.

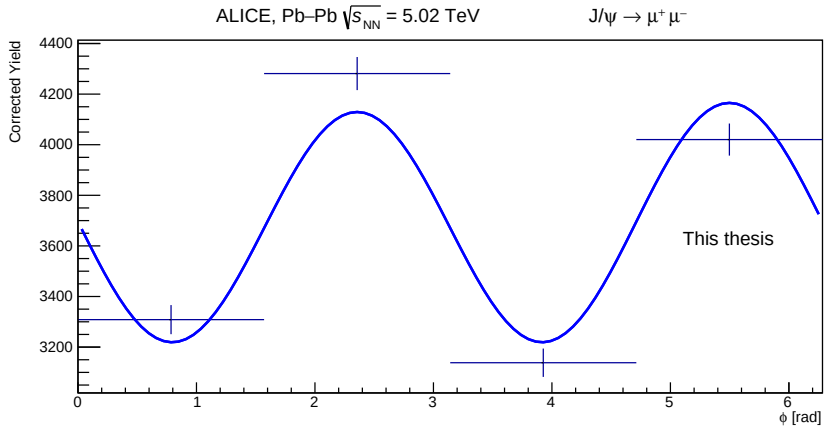

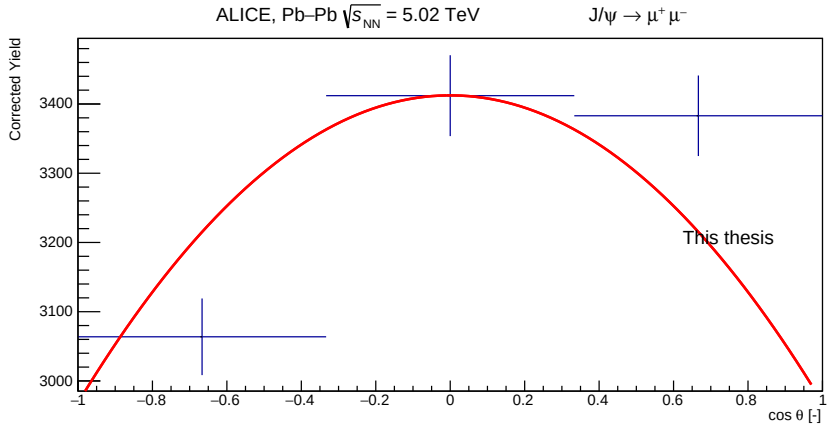

Parameter estimation of measured data

- The incoherent data sample showed reasonable results to determine the density matrix and values for polarization parameters.

$$\rho_{fit}^{incoh} = \begin{pmatrix} 0.12 & 0 & 0.23 \\ 0 & 0.43 & 0 \\ 0.23 & 0 & 0.453 \end{pmatrix} \pm \begin{pmatrix} 0.03 & 0 & 0.03 \\ 0 & 0.03 & 0 \\ 0.03 & 0 & 0.018 \end{pmatrix} (\mathrm{stat.}) \tag{10}$$

Incoherent Yield	
λ_θ	-0.25 $\pm$ 0.03
λ_ϕ	0.212 $\pm$ 0.019
$\lambda_{\theta\phi}$	-0.31 $\pm$ 0.02
$\tilde{\lambda}$	0.49 $\pm$ 0.09

Transversal		**Longitudinal**		**Unpolarized**	
λ_θ	-0.2475	λ_θ	0.6410	λ_θ	-0.02755
λ_ϕ	0.3167	λ_ϕ	-0.7934	λ_ϕ	0.03587
$\lambda_{\theta\phi}$	-0.1927	$\lambda_{\theta\phi}$	-0.5384	$\lambda_{\theta\phi}$	-0.48102
$\tilde{\lambda}$	1.0280	$\tilde{\lambda}$	-0.9709	$\tilde{\lambda}$	0.0830

Summary

- Quantum tomography provides an opportunity to study processes bypassing traditional model-dependent methods.
- Studied data sample of coherently and incoherently produced J/ψ was compared to MC generated data sample.
- The study of incoherent data sample provided reasonable results in comparison with generated incoherent transversely polarized data sample.